https://doi.org/10.2352/EI.2023.35.6.ISS-343

Color Performance of 0.8 µm CMOS Image Sensor with CMY Color Filters

An-Li Kuo, Po-Hsiang Wang, Hao-Wei Liu, Wei-Lung Tsai, Chia-Ning Hsu, Chien-Wen Lai, Yu-Chi Chang, Ching-Chiang Wu, Ken Wu; VisEra Technologies Company; No12, Dusing Rd. 1, Hsinchu Science Park, Hsinchu, Taiwan (30078).

Abstract

Modern digital cameras capture images with a subsampling method via mosaic color filter array (CFA). Of particular interest is the CFA with Cyan-Magenta-Yellow (CMY) color filters. Despite the improvement of the sensitivity, images reconstructed from CMY CFA usually suffer from lower color fidelity compared to the conventional Red-Green-Blue (RGB) color filters. In this paper, we proposed a CMY CFA with novel spectral sensitivities (CMY2.0), which were carefully designed to overcome the shortcomings of previous CMY CFA (CMY1.0) [1]. A CMY CMOS image sensor (CIS) with such optimized spectral sensitivities is then realized in order to evaluate the color performance and signal-to-noise ratio (SNR). As a result, the camera equipped with the CMY CFA with proposed spectral sensitivities (CMY2.0) features both an improved sensitivity and a high color fidelity, which is suitable for a wide range of applications, such as low-light photography, under-screen cameras and automotive cameras.

Introduction

Digital camera equipped with CMY CFAs can collect more light than RGB CFAs, which is more suitable for low-light conditions [2, 3]. However, despite the improvement of the sensitivity, images reconstructed from CMY CFA usually suffer from low color fidelity. Hence, the spectral sensitivities of the color filters should be designed to not merely collect more light but also provide good color accuracy as well so as to obtain high-quality images. Therefore, the aim of this paper is to design the optimal spectral sensitivities for CMY color filters from the perspective of color accuracy. With a view to evaluating the color performance and SNR of the CMY CFA, a CIS equipped with the optimized CMY color filters arranged in Quad Bayer structure (Figure 1) is fabricated, which can be operated in either normal mode or binning mode depending on the light conditions. With the proposed CMY color filters, the sensor features not only an improved sensitivity but also a high color fidelity, which is suitable for a wide range of applications, such as low-light photography, under-screen cameras and automotive cameras.

Method

With a view to evaluating the color performance of the next generation CMY CFA (CMY2.0), CMOS image sensors with 0.8 um pixel size using RGB, CMY1.0 and CMY2.0 color filters arranged in Quad Bayer structure (Figure 1) are fabricated, which can be operated in either normal mode or binning mode depending on the light conditions. The schematic structure of the CIS is depicted in Figure 2, where the composite metal grid structure is adopted so as to increase the pixel sensitivity and reduce the crosstalk between neighboring pixels. The sensor equipped with RGB color filters servers as a reference for comparison of color accuracy and SNR performance, whose normalized quantum efficiencies (QE) are shown in Figure 3. To improve color accuracy, the spectra of CMY are designed by referencing their corresponding XYZ values. Consequently, comparing to CMY1.0 CFA, whose normalized QE are shown in Figure 3, the spectral sensitivity of cyan color filter is designed to be wider while the spectral sensitivity of yellow color filter is designed to be red-shifted (Figure 4), where the spectral sensitivity of magenta color filter has also been modified slightly.

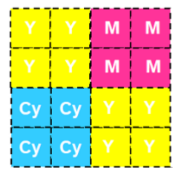

***Figure 1**. CMY sensor equipped with color filters arranged in Quad Bayer structure.*

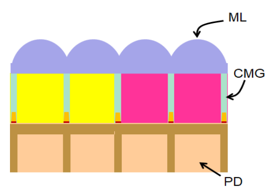

***Figure 2**. Cross sectional structure of a typical pixel in Quad Bayer arrangement equipped with yellow and magenta color filters, where each pixel is constructed with a photodiode (PD), composite metal grid (CMG), a color filter and a microlens (ML).*

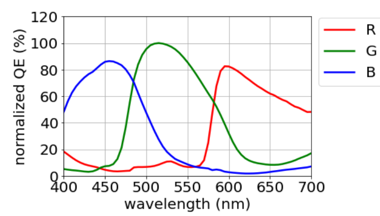

***Figure 3**. The normalized quantum efficiencies (QE) of a typical 0.8 µm CIS pixel equipped with RGB color filters in a Quad Bayer arrangement.*

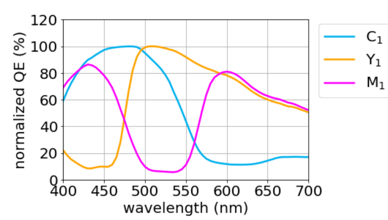

***Figure 4**. The normalized quantum efficiencies (QE) of a typical 0.8 µm CIS pixel equipped with CMY1.0 color filters in a Quad Bayer arrangement.*

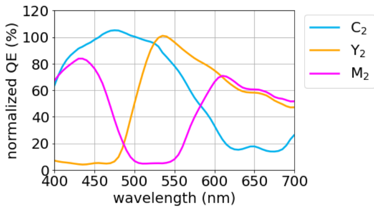

***Figure 5**. The normalized quantum efficiencies (QE) of a typical 0.8 μm CIS pixel equipped with CMY2.0 color filters in a Quad Bayer arrangement.*

Images of X-Rite ColorChecker captured by sensors equipped with RGB, CMY1.0 and CMY2.0 CFA, are shown in Figure 6, where they are illuminated by D65 under 500 lux. To reconstruct full color images, the bilateral filter for noise reduction [4], the gray-edge white balance algorithm [5], a posteriori decision demosaicing algorithm [6], color correction matrix (CCM) based method for color correction process and gamma correction process are applied to both RGB and CMY images, where the image processing pipeline is shown in Figure 7. The obtained demosaiced images before color correction process are shown in Figure 8. The color correction process is initially done in the CIELAB color space, and then converted to sRGB color space, where the reconstructed images are shown in Figure 9. To evaluate the image quality, the SNR values and the mean color differences (ΔE^*_{00}) of the 24 color patches of the X-Rite ColorChecker measured in the CIELAB color space are quantified by using Imatest Master Software.

***Figure 6**. Raw images captured by sensors equipped with (a) RGB, (b) CMY1.0 and (c) CMY2.0 CFA, which are illuminated by D65 under 500 lux.*

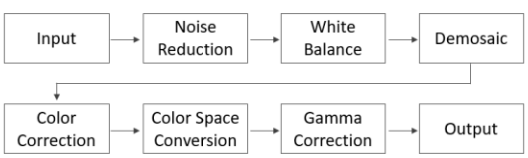

***Figure 7**. The image processing pipeline for the reconstruction of the full color images.*

***Figure 8**. Demosaicking images obtained from (a) RGB, (b) CMY1.0 and (c) CMY2.0 sensors, which are illuminated by D65 under 500 lux.*

***Figure 9**. Images reconstructed from (a) RGB, (b) CMY1.0 and (c) CMY2.0 CFA after color correction, which are illuminated by D65 under 500 lux.*

Result

Compared to the RGB CFA, both CMY1.0 and CMY2.0 CFA improve the sensitivity by 71% and 63% respectively. The minimal averaged color differences of the 24 color patches ΔE^*_{00} for RGB, CMY1.0 and CMY2.0 images are 3.0, 3.5 and 2.6 respectively, where the color accuracy of the CMY2.0 sensor is the best among all the sensors. From the color error of each color patch shown in Figure 10, one can observe that the proposed broader cyan spectral sensitivity results in better color restoration for bluish green patch while the red-shifted yellow spectral sensitivity results in better color reproduction of red and light skin color patches comparing to CMY1.0. Consequently, the color error of the enriched red patch of CMY2.0 image is now comparable to RGB image. The SNR of RGB, CMY1.0 and CMY2.0 images are 47.9, 47.1, 46.6 dB respectively. A compromise between color accuracy and SNR performance may also be lived up to RGB by adjusting the color correction matrix when processing the images. For example, in Figure 11, a high SNR value 48.1 dB of CMY2.0 image can be achieved at the cost of degradation of color accuracy, where the color error in this case is now equal to 3.17.

The color and SNR performance of the sensors under illuminant D65 with 30 lux have also been evaluated, where the reconstructed images of the RGB, CMY1.0 and CMY2.0 sensors are shown in Figure 12. The minimal averaged color differences of the 24 color patches ΔE^*_{00} for RGB, CMY1.0 and CMY2.0 images are 3.1, 3.2 and 2.7 respectively. Thus, the color error of CMY2.0 is the smallest among all the sensors. The color error for each color patch is shown in Figure 13. Again, similar to the case with those images illuminated under 500 lux, the CMY2.0 sensor has better color restoration for bluish green, red and light skin color patches comparing to CMY1.0 sensor. The SNR of RGB, CMY1.0 and CMY2.0 sensors are 34.0, 35.8, 33.3 dB respectively. By adjusting the color correction matrix of CMY2.0 sensor, the color error is then equal to 3.0 and SNR value is 34.4 dB, which is even slightly higher than the RGB sensor. Hence, a novel CMOS image sensor with high sensitivity and high color fidelity is realized.

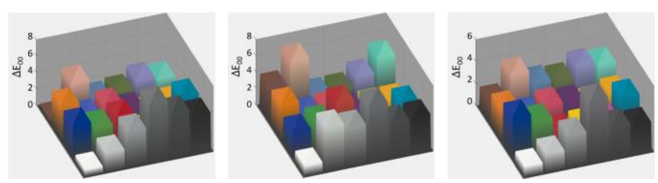

***Figure 10**. Color error ΔE^*_{00} for each color patch in X-Rite ColorChecker with the illuminant D65 under 500 lux for (a) RGB, (b) CMY1.0 and (c) CMY2.0 CFA.*

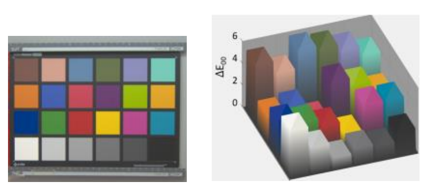

***Figure 11**. (a) A high SNR image reconstructed from CMY2.0 sensor illuminated by D65 under 500 lux and (b) color error ΔE^*_{00} for each color patch in X-Rite ColorChecker.*

Figure 12*. Images reconstructed from (a) RGB, (b) CMY1.0 and (c) CMY2.0 CFA after color correction, which are illuminated by D65 under 30 lux.*

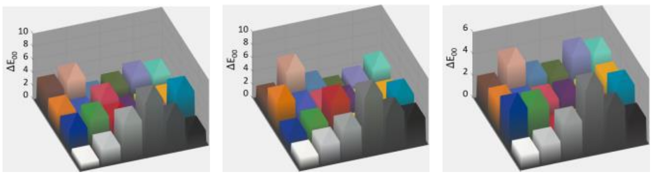

Figure 13*. Color error ΔE^*_{00} for each color patch in X-Rite ColorChecker with the illuminant D65 under 30 lux for (a) RGB, (b) CMY1.0 and (c) CMY2.0 CFA.*

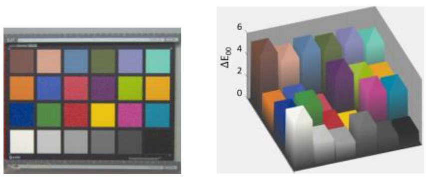

Figure 14*. (a) A high SNR image reconstructed from CMY2.0 sensor illuminated by D65 under 30 lux and (b) color error ΔE^*_{00} for each color patch in X-Rite ColorChecker.*

Conclusion

A CIS equipped with the proposed CMY2.0 CFA with high sensitivity and high color fidelity is realized, where the spectral sensitivities of the CMY color filters are designed carefully in perspective of color accuracy. The spectral sensitivity of cyan color filter is designed to be wider, which results in better color restoration for bluish green color, while the proposed red-shifted spectral sensitivity of yellow color filter results in better color restoration for red and light skin color comparing to CMY1.0 sensor. Consequently, our high sensitivity CMY2.0 sensor overcomes the shortcoming of previous CMY sensor (CMY1.0) with its superior color performance, which is suitable for a wide range of applications, such as low-light photography, under-screen cameras and automotive cameras.

References

[1] P. H. Wang, A. L. Kuo, T. Y. Ni, H. W. Liu, Y. C. Chang, C. C. Wu and K. Wu, "The study and analysis of using CMY color filter arrays for 0.8 um CMOS image sensors," in Proc. IS&T Int'l. Symp. on Electronic Imaging: Imaging Sensors and Systems, pp 201-1 - 201-3, 2022.

[2] K. Hirakawa and P. J. Wolfe, "Spatio-Spectral Color Filter Array Design for Optimal Image Recovery," in IEEE Transactions on Image Processing, vol. 17, no. 10, pp. 1876-1890, 2008.

[3] B. Sajadi, A. Majumder, K. Hiwada, A. Maki, and R. Raskar, "Switchable primaries using shiftable layers of color filter arrays," ACM SIGGRAPH 2011 papers.

[4] C. Tomasi and R. Manduchi, "Bilateral filtering for gray and color images," Sixth International Conference on Computer Vision (IEEE Cat. No.98CH36271), pp. 839-846, 1998.

[5] X. Tan, S. Lai, B. Wang, M. Zhang and Z. Xiong, "A simple gray-edge automatic white balance method with FPGA implementation," *J Real-Time Image Proc* **10**, 207–217, 2015.

[6] D. Menon, S. Andriani and G. Calvagno, "Demosaicing With Directional Filtering and a posteriori Decision," in IEEE Transactions on Image Processing, vol. 16, no. 1, pp. 132-141, 2007.